

## MODELLING THE CORONA OF HD 189733 IN 3D

A. Strugarek<sup>1</sup>, A. S. Brun<sup>2</sup>, S. P. Matt<sup>3</sup>, V. Reville<sup>2</sup>, J. F. Donati<sup>4</sup>, C. Moutou<sup>5</sup> and R. Fares<sup>6</sup>

**Abstract.** The braking of main sequence stars originates mainly from their stellar wind. The efficiency of this angular momentum extraction depends on the rotation rate of the star, the acceleration profile of the wind and the coronal magnetic field. The derivation of scaling laws parametrizing the stellar wind torque is important for our understanding of gyro-chronology and the evolution of the rotation rates of stars. In order to understand the impact of complex magnetic topologies on the stellar wind torque, we present three-dimensional, dynamical simulations of the corona of HD 189733. Using the observed complex topology of the magnetic field, we estimate how the torque associated with the wind scales with model parameters and compare those trends to previously published scaling laws.

Keywords: stars, magnetism, stellar winds

### 1 Introduction

Magnetized stellar winds have long been recognized as the major source of angular momentum extraction in main sequence stars (Parker 1958; Weber & Davis 1967; Mestel 1968). In order to reliably assess the stellar wind torque, the acceleration profile and the magnetic field geometry of the wind are required. It was recently demonstrated that, in particular, complex magnetic topologies of cool stars have a major impact on the torque (see, *e.g.* Cohen & Drake 2014; R  ville et al. 2014) compared to more simple topologies. Three dimensional numerical simulations provide a reliable way to compute, in a dynamically self-consistent way, the torque arising from stellar wind with complex magnetic fields. However, no parametrization of fully three-dimensional, non-axisymmetric stellar wind torques has yet been proposed in the literature.

We report here an ongoing effort in developing magnetohydrodynamics (MHD) simulations of the stellar winds of cool stars in three dimensions using complex magnetic field topologies. We consider one-fluid and ideal models of stellar winds which are simple compared to the most recent solar wind models (see, *e.g.*, Oran et al. 2013; Sokolov et al. 2013). However, they inherit important conservation properties from their 2.5D counterparts (see Strugarek et al. 2012, 2014b) which makes them reliable to derive general scaling laws for the stellar wind braking.

We focus, in this proceeding, on the extension of our three-dimensional stellar wind model (see Strugarek et al. 2014b) to take into account arbitrarily complex magnetic topology. As a test-bench we use the case of HD 189733 (see Section 2), which has already been modelled in 3D by Llama et al. (2013). We vary one of the free parameters of the model, the Alfv  n speed at the base of the corona (Section 3), and compare our results with previously published results. Furthermore, the various cases presented here allow us to compare the results of fully three-dimensional simulations with scaling laws that were derived in a magnetic topology-independent manner in axisymmetric geometry (R  ville et al. 2014). We find a good general agreement with this law, though the predicted torque is found to be generally larger than the one we found with our 3D models. Given that the scaling law was derived in axisymmetric geometry (in 2D), we find the general agreement satisfactory and are encouraging for further exploration of this scaling law, using fully three-dimensional numerical simulations.

---

<sup>1</sup> D  partement de physique, Universit   de Montr  al, C.P. 6128 Succ. Centre-Ville, Montr  al, QC H3C-3J7, Canada

<sup>2</sup> Laboratoire AIM Paris-Saclay, CEA/Irfu Universit   Paris-Diderot CNRS/INSU, F-91191 Gif-sur-Yvette.

<sup>3</sup> Astrophysics group, School of Physics, University of Exeter, Stocker Road, Exeter EX4 4QL, UK

<sup>4</sup> Laboratoire d'Astrophysique, Observatoire Midi-Pyr  n  es, 14 Av. E. Belin, F-31400 Toulouse, France

<sup>5</sup> Aix-Marseille Universit  , CNRS, LAM (Laboratoire d'Astrophysique de Marseille) UMR 7326, 13388 Marseille, France

<sup>6</sup> SUPA, School of Physics and Astronomy, University of St Andrews, North Haugh, St Andrews KY16 9SS, UK

## 2 Characteristics of HD 189733

The properties of the planet-hosting HD 189733 star have been reported in Bouchy et al. (2005). It is a K2V star with a mass  $M_\star = 0.82 \pm 0.03 M_\odot$  and a radius  $R_\star = 0.76 \pm 0.01 R_\odot$  (Winn et al. 2007). The rotation period of HD 189733 has been characterized by several teams using photometry (Hébrard & Lecavelier des Etangs 2006; Winn et al. 2007), and is reported between 11.8 and 13.4 days. Here we adopt a rotation period of 12 days.

We use the spectro-polarimetric magnetic maps of HD 189733 obtained by Fares et al. (2010) that were observed in July 2008 with NARVAL. We show in figure 1 the reconstructed components of the magnetic field in spherical coordinates (top to bottom) in orthographic projection viewed from the north pole (left), the equator (middle) and the south pole (right). The magnetic field is highly non-axisymmetric and derives from 20 spherical harmonics modes ( $l_{max} = 5$ ).

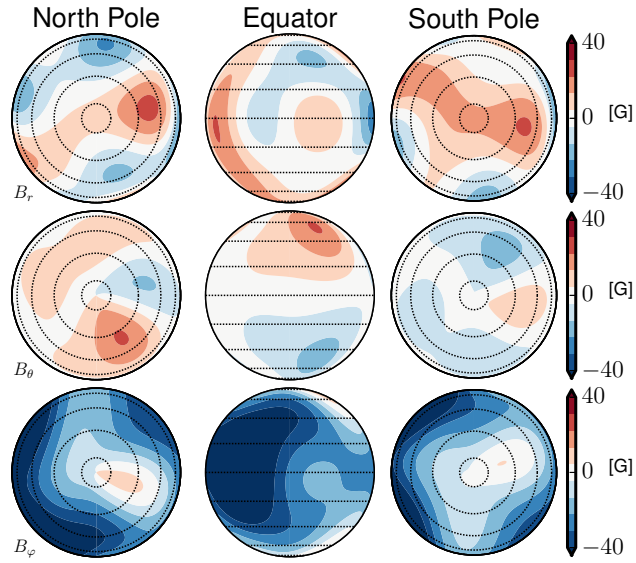


**Fig. 1.** Spectro-polarimetric reconstruction of the coronal magnetic field of HD 189733 in July 2008 (see Fares et al. 2010). The amplitude of the field is given in Gauss.

## 3 Modelling the wind of HD 189733

### 3.1 Numerical Model and Parameters

Following the work in 2.5D axisymmetric geometry described by Strugarek et al. (2014c) and in 3D by Strugarek et al. (2014b), we adapted our stellar wind model to account for the magnetic topology of observed stars. We use the PLUTO code (Mignone et al. 2007) which solves the following set of ideal MHD equations:

$$\partial_t \rho + \nabla \cdot (\rho \mathbf{v}) = 0 \quad (3.1)$$

$$\partial_t \mathbf{v} + \mathbf{v} \cdot \nabla \mathbf{v} + \frac{1}{\rho} \nabla P + \frac{1}{\rho} \mathbf{B} \times \nabla \times \mathbf{B} = \mathbf{a}, \quad (3.2)$$

$$\partial_t P + \mathbf{v} \cdot \nabla P + \rho c_s^2 \nabla \cdot \mathbf{v} = 0, \quad (3.3)$$

$$\partial_t \mathbf{B} - \nabla \times (\mathbf{v} \times \mathbf{B}) = 0, \quad (3.4)$$

where  $\rho$  is the plasma density,  $\mathbf{v}$  its velocity,  $P$  the gas pressure,  $\mathbf{B}$  the magnetic field, and  $\mathbf{a}$  is composed of the gravitational acceleration (which is time-independent) and of the Coriolis and centrifugal forces. The equations are solved in a frame rotating at the stellar rotation rate  $\Omega_\star$ . The sound speed is given by  $c_s = \sqrt{\gamma P / \rho}$ , with  $\gamma$  the ratio of specific heats. We use an ideal gas equation of state

$$\rho \varepsilon = P / (\gamma - 1), \quad (3.5)$$

where  $\varepsilon$  is the specific internal energy per mass. We use an *hll* solver combined with a *minmod* limiter. A second-order Runge-Kutta is used for the time evolution, resulting in an overall second-order accurate numerical method. The solenoidality of the magnetic field is ensured with a constrained transport method (see Mignone et al. 2012). We refer the interested reader to (Mignone et al. 2007) for an extensive description of the various numerical methods that PLUTO offers. For this first study, we use a low-resolution grid of  $224^3$  points for a domain size of  $[-20, 20]^3$ .  $96^3$  uniform grids points are used to discretize the  $[-1.5, 1.5]^3$  domain and stretched grids are used elsewhere.

The first control parameter of the modelled stellar wind is the ratio of specific heats  $\gamma$ . In order to ensure that the MHD modelling the wind produces velocities compatible with solar inferences (of the order of 400-500 km s<sup>-1</sup> at 1 AU in the case the Sun), we choose a close-to-isothermal value of  $\gamma = 1.05$ . The structure of the stellar wind is then controlled by a set of parameters that can be written as velocity ratios at the surface of the star (see, *e.g.*, Matt et al. 2012).

In this work we model the corona of HD 189733. The escape velocity at the surface of HD 189733 is  $v_{\text{esc}} = 6.41 \times 10^7$  cm/s. We choose a standard coronal temperature of  $2 \times 10^6$  K (equivalent to Llama et al. 2013) that sets the normalized sound speed at the surface of the star to  $c_s/v_{\text{esc}} = 0.29$ . The rotation period of the star is 12 days, which results in a normalized rotation velocity  $v_{\text{rot}}/v_{\text{esc}} = 5.0 \times 10^{-3}$ . Based on these parameters, the stellar wind is then driven by our boundary conditions representing the base of the corona (see Strugarek et al. 2014a,c, for complete discussions on those boundary conditions).

The last parameter controlling the stellar wind is the magnetic field. We use the radial component of the observed magnetic field (Figure 1) and perform a potential extrapolation to define the 3D magnetic field in the whole domain at initialization (see the Appendix C in Schrijver & DeRosa 2003, for a full description of the potential extrapolation technique). The magnetic field in the boundary condition –which is effectively impacting the wind driving– depends only marginally on the exact location of the source surface used for the potential extrapolation. The initial magnetic field in the whole domain is directly related to the location of the source surface, but this initial condition is rapidly modified by the wind that establishes a steady-state configuration with both open and closed field regions that is independent of the initial potential field. As a result, the choice of the source surface has no impact on our simulation results as long as it is sufficiently distant from the stellar surface.

The amplitude of the magnetic field is constrained by the observations (Figure 1), but the density at the base of the corona is not. Hence, the Alfvén speed at the base of our model is not well constrained. It can generally be related to the mass loss rate induced by the stellar wind (see Matt et al. 2012; Réville et al. 2014), which in some cases can be deduced from observations of astrospheric Ly $\alpha$  absorption (Wood 2004). However, we lack such observations for HD 189733 and are thus compelled to test a range of Alfvén speeds. We hereafter define the maximum Alfvén speed at the base of the corona by  $v_a = \max(B)/\sqrt{4\pi\rho_\star}$ , where  $B$  is the total magnetic field amplitude and  $\rho_\star$  the density at the base of the corona.  $B$  is constrained by the observations, hence we choose three different base density values  $\rho_\star \in \{1.51 \times 10^{-14}, 2.13 \times 10^{-15}, 8.3 \times 10^{-16}\}$  g cm<sup>-3</sup> that lead to the averaged velocity ratios  $v_a/v_{\text{esc}} \in \{2.58, 6.79, 11.0\}$ . The highest density we chose corresponds to the base density value chosen by Llama et al. (2013) which was tuned to reproduce the observed X-ray luminosity of HD 189733.

### 3.2 Results

In Figure 2 we show three dimensional renderings of the dynamical corona of HD 189733 for the three Alfvén velocities we considered. The blue (negative) and orange (positive) map shows the radial magnetic field at the base of the corona, where the stellar wind is driven in our model. The coronal magnetic field lines are shown in light blue, and the Alfvén surface is labelled by the transparent grey surface. We observe that for increasing base Alfvén velocity, the Alfvén surface is further away from the star, retaining a similar global shape. This is a simple consequence of the decrease of the base density in the corona: the magnetic tension strengthens compared to the inertial and pressure forces of the wind, and the magnetic field retains more closed field lines, where the coronal plasma is imprisoned and the stellar wind hindered.

We can estimate *a posteriori* the mass loss rate  $\dot{M}_w$  and angular momentum loss rate  $\dot{J}_w$  of the stellar winds. In the third case ( $v_a/v_{\text{esc}} = 11$ ), we find a mass loss rate of  $4.35 \times 10^{-13} M_\odot \text{ yr}^{-1}$ , which is very close to the mass loss rate of  $4.5 \times 10^{-13} M_\odot \text{ yr}^{-1}$  found by Llama et al. (2013). The two other cases have higher mass loss rates, respectively  $8.66 \times 10^{-12}$  and  $1.16 \times 10^{-12} M_\odot \text{ yr}^{-1}$ . Following Matt et al. (2012); Réville et al. (2014),

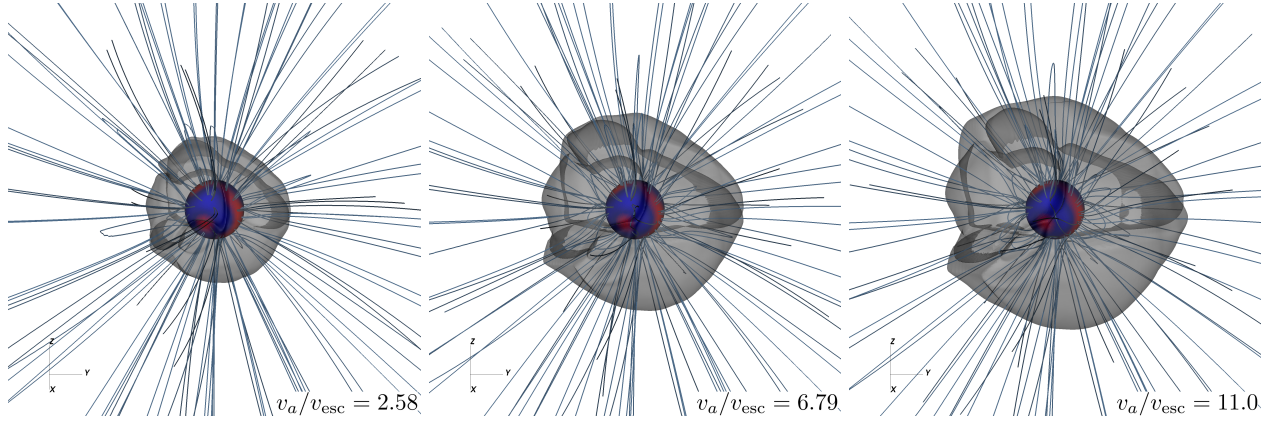


**Fig. 2.** 3D renderings of the coronal magnetic field (blue lines) of HD 189733. The color sphere shows the radial component of the magnetic field at the surface of the star. The transparent blue surface labels the Alfvén surface of the wind. From left to right,  $v_a/v_{esc}$  is 2.58, 6.79, and 11.0.

we define a torque-derived, effective Alfvén radius by relating the two loss rates through

$$\frac{R_a}{R_\star} \equiv \sqrt{\frac{-\dot{J}_w}{\dot{M}_w \Omega_\star}},$$

where  $\Omega_\star$  is the rotation rate of the star. It was recently shown by Réville et al. (2014) that this effective Alfvén radius –at least in 2.5D axisymmetric models– can be related to the wind magnetization parameter

$$\Upsilon_o \equiv \frac{\Phi_o^2}{R_\star^2 \dot{M}_w v_{esc}},$$

where the open magnetic flux is given by

$$\Phi_o = \int_S |\mathbf{B} \cdot d\mathbf{S}|,$$

where  $\int_S \cdot d\mathbf{S}$  stand for the integral over a closed surface at a sufficiently large distance from the central star for the magnetic field lines to be all open. The average Alfvén radius and the magnetic confinement parameter are related through

$$\frac{R_a}{R_\star} = K_3 \left[ \frac{\Upsilon_o}{\sqrt{1 + (f/K_4)^2}} \right]^m \quad (3.6)$$

where the coefficients  $K_3$ ,  $K_4$  and  $m$  were determined empirically by Réville et al. (2014) to be  $K_3 = 1.4 \pm 0.1$ ,  $K_4 = 0.06 \pm 0.01$  and  $m = 0.31 \pm 0.02$ .

We compute  $R_a$  and  $\Upsilon_o$  in our three models and display them in Figure 3. The scaling law predicted by Réville et al. (2014) is shown by the black line. The grey area labels the error bars of this scaling law. Our cases seem to follow roughly the scaling-law trend, but appear to be shifted downwards. This is in reality awaited since our reference scaling law was derived with a fixed sound speed ratio of  $c_s/v_{esc} = 0.222$  (see Réville et al. 2014). In our case, we consider a much larger sound speed  $c_s/v_{esc} = 0.2913$ . By simply multiplying the  $K_3$  coefficient (see equation (3.6)) by 0.65 (close to the ratio of the sound speed considered by Réville et al. (2014) and the one considered here), our results are nicely reconciled with the predicted scaling-law (red dashed line and red area). The power-law trend that was derived from axisymmetric models with only three different topologies (Réville et al. 2014) seems to apply, at least at first order, to non-axisymmetric topologies involving numerous spherical harmonics modes.

## 4 Conclusions

We have presented a set of simulations to model the coronal structure around distant stars based on observed magnetic maps. We applied this method to the case of HD 189733. Due to the lack of constraints on the

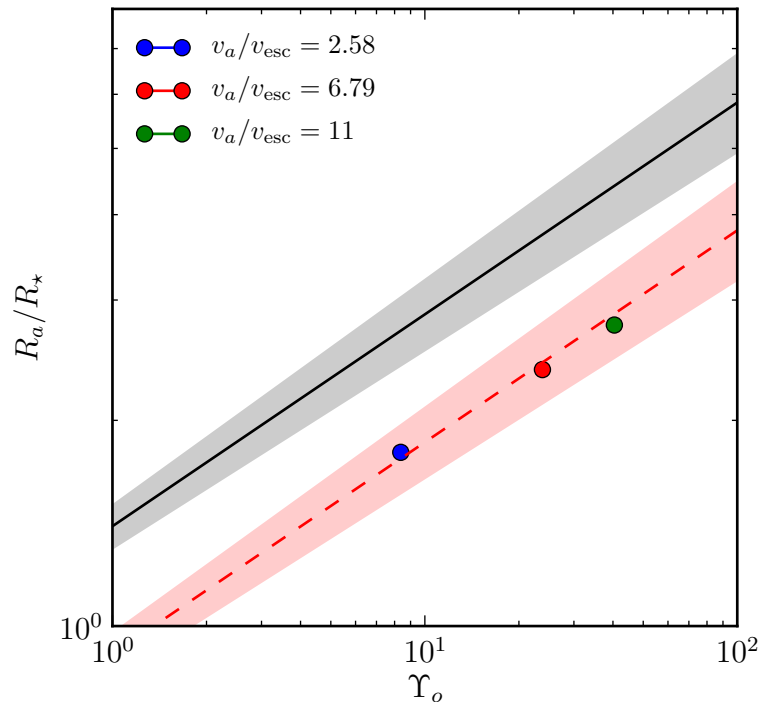


**Fig. 3.** Generalized Alfvén radius as a function of the wind magnetization parameter  $\Upsilon_o$  (see text). The black line and grey area show the scaling law prediction from Réville et al. (2014). The dashed red line and red area represent the same scaling law, modified to account a different sound speed at the base of the corona.

mass loss rate of the star, models of the stellar wind of HD 189733 have free parameters, which we varied to explore their impact on the coronal structure, and on the mass and angular momentum loss rates of the star. In spite of the low resolution we used, and the complexity of the magnetic field topology, we find a good general agreement with the torque scaling law that was derived in 2.5D geometry by Réville et al. (2014) and our results compare very well with previous models of the corona of HD 189733 (Llama et al. 2013). Nevertheless, the slight discrepancies compared to the predicted torque scaling law warrant higher-resolution runs. Furthermore, HD 189733 is a slow-rotator; we intend to confirm the torque scaling law with three-dimensional simulations in the rapid-rotator regime as well in a near future.

HD 189733 is known to harbor a close-in Jupiter-like planet, HD 189733b, which orbits at 0.031 AU around its host ( $R_p = 1.15 R_J$  and  $M_p = 1.13 M_J$ , see Boisse et al. 2009). It was recently suggested that due to its proximity, HD 189733b could possess a variable-size bow-shock along its phase, which could in principle be detected in near-UV transit lights (Llama et al. 2013). Such observations would then be extremely useful to better constrain stellar wind models. The wind model we presented here is a first step toward the global modelling of the star-planet system in the spirit of Cohen et al. (2014); Strugarek et al. (2014c).

AS thank A. Vidotto for discussions about the modelling of the corona of HD 189733. This work was supported by the ANR 2011 Blanc Toupies and the ERC project STARS2 (207430). The authors acknowledge CNRS INSU/PNST and CNES/Solar Orbiter fundings. AS acknowledges support from the Canada’s Natural Sciences and Engineering Research Council and from the Canadian Institute of Theoretical Astrophysics (National fellow). We acknowledge access to supercomputers through GENCI (project 1623), Prace, and ComputeCanada infrastructures.

## References

- Boisse, I., Moutou, C., Vidal-Madjar, A., et al. 2009, *A&A*, 495, 959  
 Bouchy, F., Udry, S., Mayor, M., et al. 2005, *A&A*, 444, L15  
 Cohen, O. & Drake, J. J. 2014, *ApJ*, 783, 55

- Cohen, O., Drake, J. J., Gloer, A., et al. 2014, *ApJ*, 790, 57
- Fares, R., Donati, J.-F., Moutou, C., et al. 2010, *MNRAS*, 406, 409
- Hébrard, G. & Lecavelier des Etangs, A. 2006, *A&A*, 445, 341
- Llama, J., Vidotto, A. A., Jardine, M., et al. 2013, *MNRAS*, 2442
- Matt, S. P., MacGregor, K. B., Pinsonneault, M. H., & Greene, T. P. 2012, *ApJ*, 754, L26
- Mestel, L. 1968, *MNRAS*, 138, 359
- Mignone, A., Bodo, G., Massaglia, S., et al. 2007, *ApJS*, 170, 228
- Mignone, A., Zanni, C., Tzeferacos, P., et al. 2012, *The Astrophysical Journal Supplement*, 198, 7
- Oran, R., van der Holst, B., Landi, E., et al. 2013, *ApJ*, 778, 176
- Parker, E. N. 1958, *ApJ*, 128, 664
- Réville, V., Brun, A. S., Matt, S. P., & Strugarek, A. 2014, submitted to *ApJ*
- Schrijver, C. & DeRosa, M. 2003, *Sol. Phys.*, 212, 165
- Sokolov, I. V., van der Holst, B., Oran, R., et al. 2013, *ApJ*, 764, 23
- Strugarek, A., Brun, A. S., & Matt, S. 2012, in *SF2A-2012: Proceedings of the Annual meeting of the French Society of Astronomy and Astrophysics*. Eds.: S. Boissier, 419–423
- Strugarek, A., Brun, A. S., Matt, S. P., & Réville, V. 2014a, *Nature of Prominences and their role in Space Weather*, 300, 330
- Strugarek, A., Brun, A. S., Matt, S. P., & Réville, V. 2014b, *th Cambridge Workshop on Cool Stars, Stellar Systems, and the Sun, Proceedings of Lowell Observatory*, 1
- Strugarek, A., Brun, A. S., Matt, S. P., & Réville, V. 2014c, *ApJ*, 795, 86
- Weber, E. J. & Davis, L. J. 1967, *ApJS*, 148, 217
- Winn, J. N., Holman, M. J., Henry, G. W., et al. 2007, *The Astronomical Journal*, 133, 1828
- Wood, B. E. 2004, *Liv. Rev. Sol. Phys.*, 1, 2